Rings and Things

David Ormrod Morley

Balliol College

University of Oxford

A thesis submitted for the degree of

Doctor of Philosophy

Trinity 2020

Contents

List of Notes By David

List of Notes By Mark

1 | Network Theory

The theory underpinning complex networks is discussed, covering the representation of atomic systems as networks and the relationship of the dual network to ring structure. The laws which govern the topological properties of physical networks, namely Euler's law, Lemaître's law and the Aboav-Weaire law are also introduced.

1.1 Network Theory

The scope of what constitutes a complex network is extremely broad, covering everything from the tangible (*e.g.* computational clusters) to the more abstract (*e.g.* social interactions). Yet part of the appeal and power of network science is the ability to quantify and relate these highly disparate systems with the same underlying theory. A network is simply a collection of components termed *nodes* and the connections between them termed *links*, an example of which is given in figure 1.1. There are then two fundamental classes of network based on the nature of the connections. Networks in which the links between nodes are mutual are termed undirected, whereas those in which the links are one-way are termed directed [52]. At the risk of dating this thesis, this is the difference between Facebook (an undirected social network of friends) and Twitter (a directed social network of followers). All the networks considered in this work are undirected and all the theory assumes this property.

1.1.1 Node Degree and Probability Distributions

??

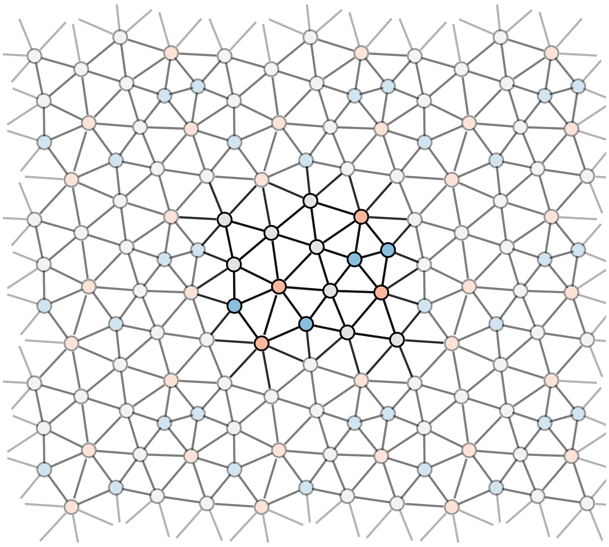

Figure 1.1: Example of a periodic two-dimensional network where nodes are represented by circles and links as lines. Nodes are coloured similarly according to their degree, whilst periodic images are greyed out to highlight the central repeating unit.

A key concept in network science is the the node degree, defined as the number of links that each node possesses. A node with k links is then said simply to have degree k, where $k \in \mathbb{N}$. This is illustrated in figure 1.1, which consists of 5- (blue), 6- (grey) and 7- (red) degree nodes. The occurrence and correlations of nodes of given degrees can then be described by a range of probability distributions.

The probability of a randomly selected node having degree k is given by the node degree distribution, denoted p_k. This is a normalised discrete distribution such that

$$\sum_k p_k = 1\,. \tag{1.1}$$

The n^{th} moments of this distribution are then given by:

$$\langle k^n \rangle = \sum_k k^n p_k\,. \tag{1.2}$$

Alternatively, one can also calculate the probability that a randomly selected link has a k-degree node at the end, denoted q_k. This is not the same as the distribution above, as there is greater chance of selecting links which emanate from high degree nodes, in a manner which is proportional to the node degree. As this distribution is normalised, this leads to the relations:

$$\sum_k q_k = 1 \tag{1.3}$$

$$q_k = \frac{kp_k}{\langle k \rangle}\,. \tag{1.4}$$

In addition, one can also evaluate the probability that a randomly chosen link has nodes of degree j,k at either end. This is the node joint degree distribution, denoted e_{jk}. Once again this is normalised and satisfies the following relationships:

$$\sum_{jk} e_{jk} = 1, \tag{1.5}$$

$$\sum_{jk} e_{jk} = q_j \tag{1.6}$$

$$e_{jk} = e_{kj}\,, \tag{1.7}$$

where the final result arises from reciprocal nature of the links in an undirected network. As an example, these three probability distributions are provided for the network in figure 1.1:

$$\mathbf{p} = \frac{1}{16}\begin{array}{c c}\begin{bmatrix}4\\8\\4\end{bmatrix} & \begin{array}{c}5\\6\\7\end{array}\end{array} \qquad \mathbf{q} = \frac{1}{96}\begin{array}{c c}\begin{bmatrix}20\\48\\28\end{bmatrix} & \begin{array}{c}5\\6\\7\end{array}\end{array} \qquad \mathbf{e} = \frac{1}{96}\begin{array}{c c}\begin{array}{ccc}5 & 6 & 7\end{array} & \\ \begin{bmatrix}2 & 9 & 9\\ 9 & 22 & 17\\ 9 & 17 & 2\end{bmatrix} & \begin{array}{c}5\\6\\7\end{array}\end{array}\,. \tag{1.8}$$

1.1.2 Atomic and Ring Networks

To see how network theory relates to atomic materials, consider the amorphous graphene configuration in figure 1.2a. In this network the nodes represent carbon atoms and the links sp^2 bonds. The node degree in the atomic network for all nodes is then equal to three, being equivalent to the atomic coordination number (which throughout this thesis will be denoted by c). This is problematic, because whilst there is clear disorder in the system, it is not well captured by the atomic network. Due to the fact that the local environment around the atoms is identical, when examining say the node degree distribution any information about the glassy structure is lost. This network is to first order indeterminable from a crystalline hexagonal lattice.

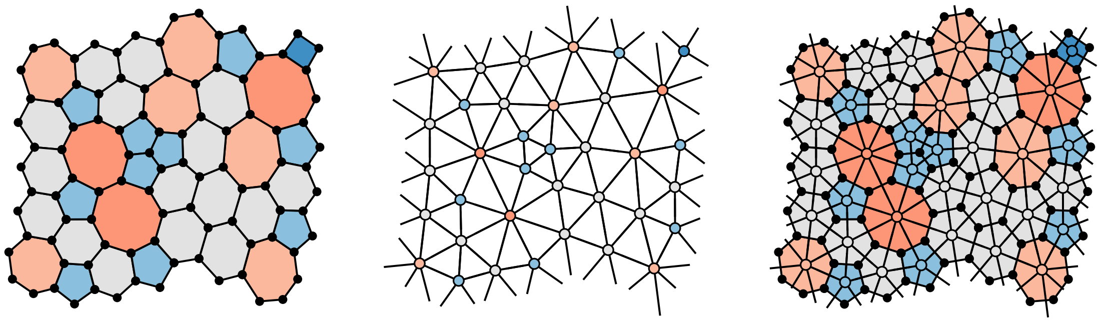

(a) Atomic network. (b) Ring network. (c) Dual relationship.

Figure 1.2: Panel (a) gives an example of a 3- coordinate periodic atomic network with disordered ring structure. Nodes and links represent atoms and bonds respectively where rings are coloured by size. Panel (b) gives the corresponding ring network where nodes and links represent rings and their adjacencies, where nodes are coloured by degree. Panel (c) shows the dual relationship between the atomic and ring networks, where the node degree in the ring network is equal to the ring size in the atomic network.

Observing figure 1.2a one can see there is another level of structure in the network, namely that of the ring structure. A ring is strictly any closed path of sequentially linked nodes in a network, but this thesis will use the term in reference only to the primitive rings *i.e.* those which cannot be subdivided into two smaller rings [53]. A ring of size k (or k-ring) is then defined as a ring with k constituent nodes. It is clear that finding and counting the number of rings of each size, often termed calculating the ring statistics, does then quantify the disorder in the system [29]. The ring statistics can be summarised by the normalised probability distribution, p_k.

However, there is a more efficient way of representing and quantifying the ring structure in the system, and that is by constructing the dual network [54]. The dual is generated by placing a node at the centre of each ring and linking the nodes of adjacent (*i.e.* edge-sharing) rings, as can be seen in figure 1.2b. This will be referred to as the ring network. The ring network is a reciprocal lattice in which the node degree, k, is equivalent to the ring size in the atomic network. Similarly, it consists solely of triangles, reflecting the 3-coordinate nature of the underlying atomic network. Hence, the disorder is captured directly in the node properties of the ring network. These characteristics make the ring network preferable for manipulating and analysing the systems in this thesis.

1.2 Topological Laws

There are a number of laws which govern the topological properties of two-dimensional network-forming materials. These laws constrain the ring structure, influencing the network properties in a manner that makes physical networks unique in the field of network science. These laws act on a number of "levels": Euler's law controls the overall mean ring size, Lemaître's law the ring size distribution and the Aboav-Weaire law the ring-ring correlations.

1.2.1 Euler's Law

Euler's law constrains the mean ring size, $\langle k \rangle$, in an atomic network or equivalently the mean node degree of the ring network. The atomic networks studied in this work are all two-dimensional, connected (there is a path between any two nodes) and planar (they have no overlapping links) and so are subject to Euler's formula which states:

$$N + V - E = \chi, \tag{1.9}$$

where N, V, E are the number of rings, vertices and edges in the network and χ in an integer termed the Euler characteristic, which is dependent on the global topology of the system. Each vertex represents an atom and the number of edges emanating from each vertex is then the coordination number.

For generality consider an atomic network with atoms of assorted coordination numbers, c. If the proportion of each coordination type is x_c, then the mean coordination number is given by $\langle c \rangle = \sum_c c x_c$. This allows the number of edges to be written in terms of the number of vertices as $E = \frac{V}{2}\langle c \rangle$. In turn the mean ring size is simply the total number of vertices per ring, allowing for multiple counting, such that $\langle k \rangle = \frac{V}{N}\langle c \rangle$. Substituting these two expressions into equation (1.9) leads to the expression:

$$\langle k \rangle = \frac{2\langle c \rangle \left(1 - \chi/N\right)}{\langle c \rangle - 2}. \tag{1.10}$$

Hence the average node degree in the ring network (equivalent to the mean ring size of the physical network), is simply related to the average degree of the physical network (*i.e.* local coordination environment), the topology of the system and the number of rings.

Although equation (1.10) may appear simple, it is a very powerful constraint. To demonstrate this consider a two-dimensional lattice with two possible coordination environments $c = 3, 4$. The planar case with periodic boundary conditions (mimicking an infinite planar lattice) maps onto the torus with $\chi = 0$, and so:

$$\langle k \rangle = \begin{cases} 6, & x_3 = 1 \\ 4, & x_4 = 1 \\ 5, & x_3 = 2/3, x_4 = 1/3 \end{cases} . \tag{1.11}$$

To reiterate in plain terms, this means that if there is a material consisting of atoms all forming exactly three bonds (as for amorphous carbon), the mean ring size *must* be equal to six. Similarly if all atoms form four bonds the mean ring size is four, and if there is a two-thirds to one-third mixture of coordination environments the mean ring size is five. The simplest illustrations of these are the hexagonal, square and cairo regular tilings, shown in figure 1.3, but this law holds equally well for amorphous configurations. For aperiodic systems strictly $\chi = 1$, but as $N \to \infty$, the proportion of vertices with unsatisfied coordination on the sample perimeter become negligible overall as does the term in χ. Therefore in reality these relationships hold, and remain as applicable to amorphous graphene as the basalt columns in Fingal's Cave, and the Penrose tiling [37, 55].

This analysis also extends to spherical topology where $\chi = 2$, and so:

$$\langle k \rangle = \begin{cases} \frac{6N-12}{N}, & x_3 = 1 \\ \frac{4N-8}{N}, & x_4 = 1. \end{cases} \tag{1.12}$$

These relationships are the origin of the 12 pentagon rule for 3-coordinate fullerenes (the "football problem"), or equivalently an "8 triangle rule" in the 4-coordinate case, as this is the only way to satisfy these equations if the allowed ring sizes are limited to $k = 5, 6$ and $k = 3, 4$ respectively (as in figures 1.3d, 1.3e) [56]. Much of the richness in the behaviour of two-dimensional physical networks stems from this fundamental constraint on the network average degree.

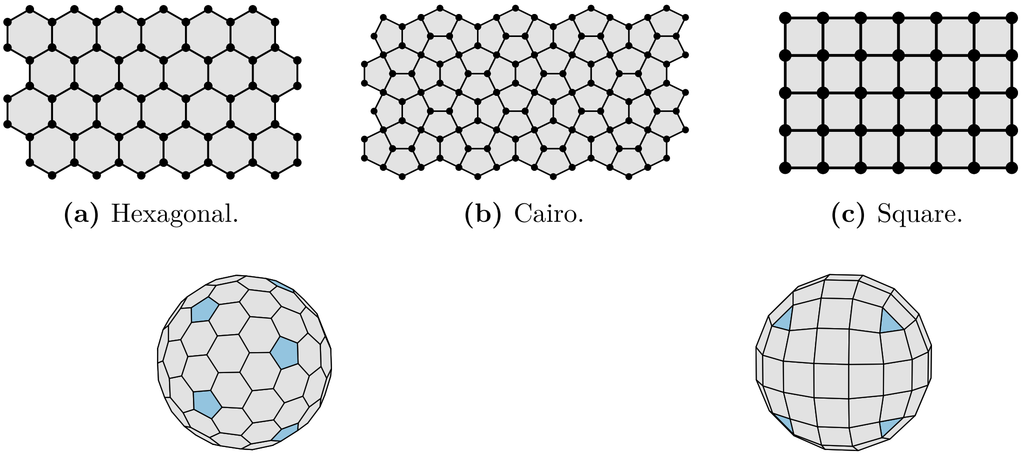

(a) Hexagonal. **(b)** Cairo. **(c)** Square.

(d) 3-coordinate fullerene. **(e)** 4-coordinate fullerene.

Figure 1.3: Panels (a)-(c) give regular planar tilings of 6-, 5- and 4- rings, where the ring size is related to the underlying atomic coordination. Panels (d) and (e) show the 3- and 4- coordinate tilings in spherical topology, where the mean ring size is reduced due to the change in the Euler characteristic.

1.2.2 Lemaître's Law

Knowing that the mean node degree is fixed by Euler's law, the next level of available information is the form of the underlying degree distribution, p_k. Interestingly, the degree distributions found in physical ring networks seem relatively well defined. For instance, it has been noted in models and realisations of two-dimensional silica glass that the ring statistics looked to follow a lognormal distribution [11, 15]. Lemaître *et al.* demonstrated that the distribution in 3-coordinate networks systems can be well described by a maximum entropy distribution [57]. Lemaître's maximum entropy method is summarised here, trivially extended to arbitrary coordination.

The entropy of a probability distribution is defined as

$$\mathcal{S} = -\sum_k p_k \log p_k. \tag{1.13}$$

In addition, the degree distribution has the following constraints:

$$\sum_k p_k = 1, \tag{1.14}$$

$$\sum_k k p_k = \langle k \rangle, \tag{1.15}$$

$$\sum_k \frac{p_k}{k} = \text{constant}, \tag{1.16}$$

where the first two constraints correspond to the normalisation condition and the fixed mean ring size, and the final constraint will be discussed below. The entropy can then be maximised using Lagrange's method of undetermined multipliers to yield the result:

$$p_k = \frac{e^{-\lambda_1 k - \lambda_2/k}}{\sum_k e^{-\lambda_1 k - \lambda_2/k}}, \tag{1.17}$$

which can be solved numerically by substitution into equations (1.15),(1.16). By allowing the chosen constant to vary, a family of maximum entropy curves can be generated, as in figure 1.4a. The resulting distributions can be summarised by relating the variance, $\mu_2 = \langle k^2 \rangle - \langle k \rangle^2$, to a single chosen node degree probability, leading to the plot known as Lemaître's law, given in figure 1.4b. It is usually framed in the context of the proportion of hexagons in a system, p_6, for the precise reason that most networks have $\langle k \rangle = 6$ and p_6 as the largest contribution. Many experimental and theoretical studies have shown good agreement to this law [58–60].

Simple extensions of the classic law are however possible, by modifying the mean degree or the permitted degree range. For instance, k is usually taken in the interval $k \geq 3$ (as the triangle, $k = 3$, is the smallest polygon), but there can be manifestations of physical systems where only certain degrees are accessible [61]. Additional examples of such systems will be procrystalline lattices explored in chapter **??**. The resulting Lemaître curves for a selection of these modifications are given in figure 1.4c. A discussion of these will be recur throughout this thesis, but one can see that the application of the allowable ring size constraints leads to marked differences in the maximum entropy solutions. The maximum value of these curves can be simply determined by removing constraint (1.16), equivalent to setting $\lambda_2 = 0$ in equation (1.17).

The only somewhat puzzling aspect of this successful theory is the choice of constraint (1.16). It was originally rationalised on the basis that the areas of rings of a given size, A_k, can be well fit by an expression $A_k = ak + b + c/k$, where a, b and c are constants. As noted at the time, this is by no means true for all systems and in fact is contrary to the widely known Lewis law, which states that A_k is linear in k

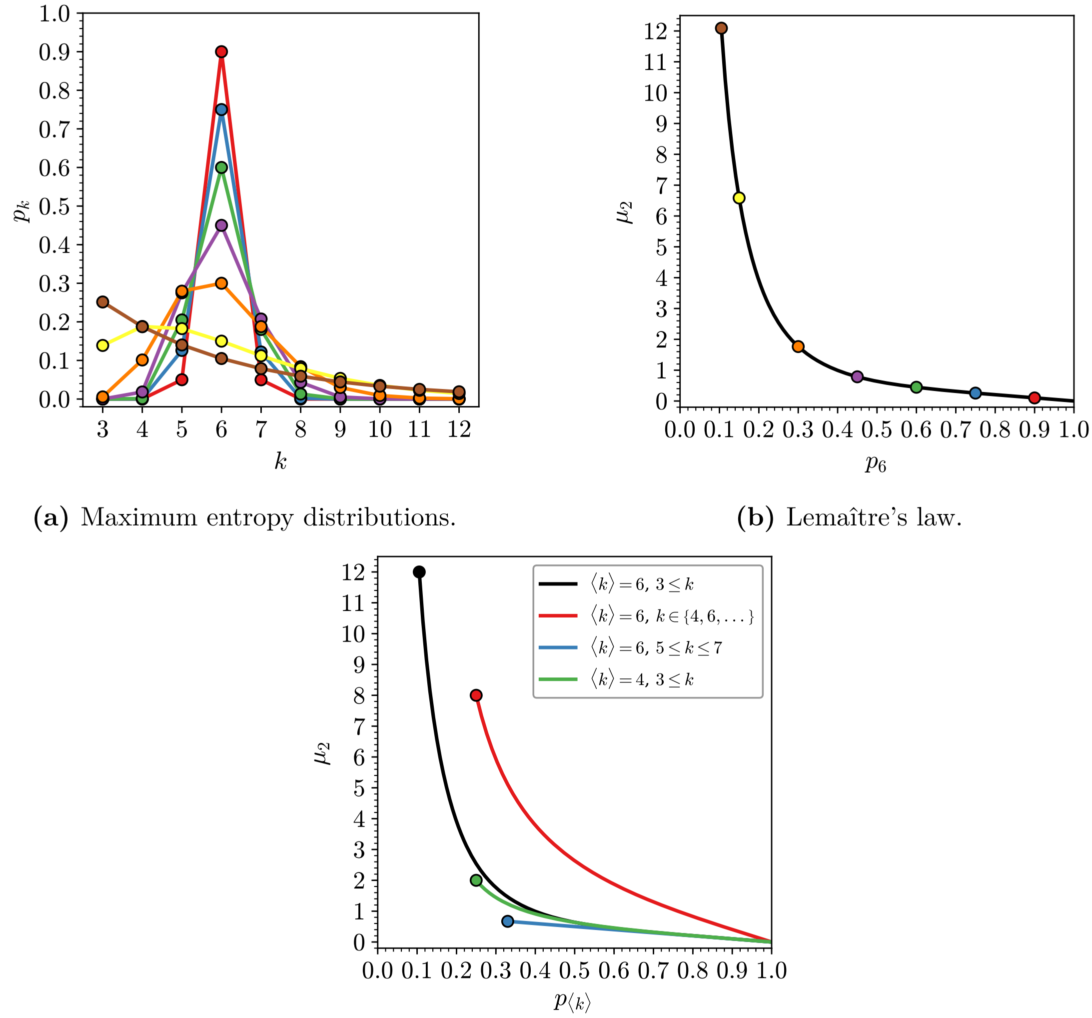

(a) Maximum entropy distributions.

(b) Lemaître's law.

(c) Extensions to Lemaître's law.

Figure 1.4: Illustration of Lemaître's maximum entropy method. Panel (a) gives examples of explicit maximum entropy distributions with different values of p_6. Panel (b) shows how these distributions can be summarised in a plot of p_6 *vs.* μ_2 (Lemaître's law). Panel (c) provides extensions to the law by modifying the underlying constraints of the mean ring size and allowable k-range.

for many observable networks [62–64]. Despite this, the universality of the Lemaître law suggests that there must be a physical basis to (1.16), and in the section **??** it will be demonstrated that it can be regenerated by considering ring adjacencies.

1.2.3 Aboav-Weaire Law

The ring statistics given by Lemaître's law are an important measure for physical networks, but they do not provide a complete characterisation of the ring structure, as they say nothing about the ring adjacencies. This is important because whilst with the same ring statistics it is theoretically possible to organise the rings in many different arrangements, it is well known experimentally that only a subsection of these are observed. The vast majority of physical systems have a preference for small rings ($k < \langle k \rangle$) be adjacent to large rings ($k > \langle k \rangle$). This effect was first noted in the grains of polycrystals by Aboav [18]. Aboav quantified these ring correlations by measuring the mean ring size about a k-ring, denoted m_k, and found empirically that $m_k \approx 5 + 8/k$.

In an attempt to explain this observation, Weaire came across the following relation

$$\sum_k k m_k p_k = \sum_k k^2 p_k = \mu_2 + \langle k \rangle^2 \,, \tag{1.18}$$

known as Weaire's sum rule [19]. From this he suggested the modification of $m_k = 5 + (6 + \mu_2)/k$ which satisfied this rule. Aboav's original equation then became a special case when $\mu_2 = 2$, which is close to the expected value for a random collection of Voronoi polygons (see section ??). Aboav then proposed that if a generic form of $m_k = A + B/k$ was used in conjunction with Weaire's sum rule then

$$m_k = A + \frac{\mu_2 + \langle k \rangle^2 - A\langle k \rangle}{k} \,. \tag{1.19}$$

This is now more commonly expressed in the linear form [65]:

$$k m_k = \mu_2 + \langle k \rangle^2 + \langle k \rangle (1 - \alpha)(k - \langle k \rangle) \,. \tag{1.20}$$

Equation 1.20 is known as the Aboav-Weaire law and relates the mean ring size about a given central ring to a single fitting parameter, α. The value of α describes the strength of the ring correlations, with a larger positive value indicating a greater tendency for small-large ring adjacencies. More specifically, the random limit can be deduced by evaluating $\frac{\partial m_k}{\partial x} = 0$ as [66]:

$$\alpha = -\frac{\mu_2}{\langle k \rangle^2} \,. \tag{1.21}$$

Hence all systems with $\alpha > -\mu_2/\langle k \rangle^2$ have more small-large ring adjacencies than would be expected from chance whilst conversely those with $\alpha < -\mu_2/\langle k \rangle^2$ have more small-small and large-large pairings.

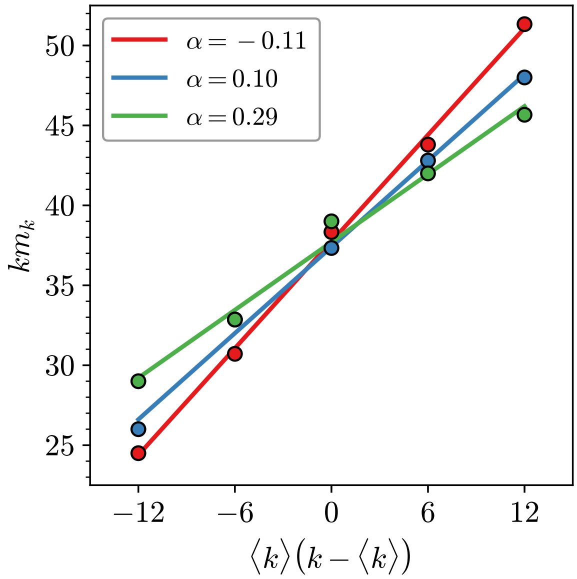

Figure 1.5: Calculation of an Aboav-Weaire fit for three configurations (shown in figure **??**(b)-(d)). The value of the α parameter quantifies the tendency of small rings to be adjacent to large rings, with a larger value indicating stronger small-large ring correlations.

Despite the Aboav-Weaire law being purely empirical and there being no topological requirement for m_k to vary systematically k, the law does seem to hold well for a diverse set of physical systems. The law is well used for example in studies of materials, emulsions, biological tissues as well as in planetary science [28, 67–70]. As an example of the calculation of the Aboav-Weaire parameter, the plots of the fits for the systems in figure **??** are presented in figure 1.5, along with the corresponding α parameters. This demonstrates two contrasting aspects of the Aboav-Weaire law. Firstly the law holds very well, especially given the fact that these samples consist of just twenty rings each. However, it also demonstrates that the law is by no means exact and that some greyness is inevitably introduced during the linear regression.

Appendices

A | Calculation of Forces

The calculation of forces from a given potential model is central to the geometry optimisation routines (see section **??**) employed in many algorithms in this thesis. This appendix derives the equations used to calculate the forces for the potentials covered throughout this work. The notation used will aim to be consistent, and is outlined as follows. A position vector is denoted by $\mathbf{r} = [x\,y]^T$, with:

$$\mathbf{r_{ij}} = \mathbf{r_j} - \mathbf{r_i}\,, \tag{A.1}$$

$$r_{ij} = |\mathbf{r_{ij}}|\,, \tag{A.2}$$

$$\mathbf{\hat{r}_{ij}} = \frac{\mathbf{r_{ij}}}{r_{ij}}\,. \tag{A.3}$$

The derivative of a function with respect to $\mathbf{r}$ is then given by $\frac{\partial f(\mathbf{r})}{\partial \mathbf{r}} = \left[\frac{\partial f(\mathbf{r})}{\partial x}\ \frac{\partial f(\mathbf{r})}{\partial y}\right]^T$. It therefore follows that:

$$\frac{\partial r_{ij}}{\partial \mathbf{r_{ij}}} = \mathbf{\hat{r}_{ij}}\,, \quad \frac{\partial r_{ij}}{\partial \mathbf{r_i}} = -\mathbf{\hat{r}_{ij}}\,, \quad \frac{\partial r_{ij}}{\partial \mathbf{r_j}} = \mathbf{\hat{r}_{ij}}\,. \tag{A.4}$$

Angles are denoted by θ_{ijk}, representing the angle between $\mathbf{r_{ij}}$ and $\mathbf{r_{ik}}$. It will also be useful to determine the derivative of the cosine of angles with respect to a position vector:

$$\begin{aligned}
\frac{\partial \cos\theta_{ijk}}{\partial \mathbf{r_j}} &= \frac{\partial}{\partial \mathbf{r_j}}\left(\frac{\mathbf{r_{ij}}\cdot\mathbf{r_{ik}}}{r_{ij}r_{ik}}\right) \\
&= \frac{r_{ij}r_{ik}\mathbf{r_{ik}} - \mathbf{r_{ij}}\cdot\mathbf{r_{ik}}\mathbf{\hat{r}_{ij}}\mathbf{r_{ik}}}{r_{ij}^2 r_{ik}^2} \\
&= \frac{1}{r_{ij}}\left(\mathbf{\hat{r}_{ik}} - \mathbf{\hat{r}_{ij}}\cdot\mathbf{\hat{r}_{ik}}\mathbf{\hat{r}_{ij}}\right) \\
&= \frac{1}{r_{ij}}\left(\mathbf{\hat{r}_{ik}} - \cos\theta_{ijk}\mathbf{\hat{r}_{ij}}\right)\,,
\end{aligned} \tag{A.5}$$

and similarly

$$\frac{\partial \cos\theta_{ijk}}{\partial \mathbf{r_k}} = \frac{1}{r_{ik}} \left(\hat{\mathbf{r}}_{\mathbf{ij}} - \cos\theta_{ijk} \hat{\mathbf{r}}_{\mathbf{ik}} \right) . \tag{A.6}$$

These relationships form the basis to derive the forces for the various stretching and angular potentials used in this thesis.

The force on a given particle at $\mathbf{r_i}$ is given by the negative derivative of the potential:

$$\mathbf{F_i} = -\frac{\partial \mathcal{U}}{\partial \mathbf{r_i}} . \tag{A.7}$$

As forces are conservative, the sum of the forces on all particles must be zero *i.e.* for stretching and angular terms respectively:

$$\mathbf{F_i} = -\mathbf{F_j} , \tag{A.8}$$

$$\mathbf{F_i} = -\mathbf{F_j} - \mathbf{F_k} . \tag{A.9}$$

In the following sections K denotes a force constant and a subscript zero an equilibrium value.

A.1 Harmonic Stretching Potential

The harmonic stretching potential is a simple bonding potential that approximates many atomic potentials at small displacements. The interaction between two particles at separation $\mathbf{r_{ij}}$ is given by:

$$\mathcal{U} = \frac{K}{2} \left(r_{ij} - r_0 \right)^2 . \tag{A.10}$$

The forces are therefore:

$$\mathbf{F_j} = -\frac{\partial \mathcal{U}}{\partial r_{ij}} \frac{\partial r_{ij}}{\partial \mathbf{r_j}} = -K \left(r_{ij} - r_0 \right) \hat{\mathbf{r}}_{\mathbf{ij}} , \tag{A.11}$$

with $\mathbf{F_i}$ given by equation (A.8).

A.2 Quartic Stretching Potential

The quartic stretching potential is related to the harmonic potential, but is even more computationally efficient as there is no square root operations are required. The interaction between two particles at separation $\mathbf{r_{ij}}$ is given by:

$$\mathcal{U} = \frac{K}{4}\left(r_{ij}^2 - r_0^2\right)^2 . \tag{A.12}$$

The forces are therefore:

$$\mathbf{F_j} = -\frac{\partial \mathcal{U}}{\partial r_{ij}}\frac{\partial r_{ij}}{\partial \mathbf{r_j}} = -K\left(r_{ij}^2 - r_0^2\right)\mathbf{r_{ij}} , \tag{A.13}$$

with $\mathbf{F_i}$ given by equation (A.8).

A.3 Harmonic Cosine Angle Potential

In analogue with the stretching potential, the harmonic cosine angle is a elegant yet simple form angular potential, utilising the cosine function to reduce overheads when calculating angles. The interaction between three particles with angle θ_{ijk} is given by:

$$\mathcal{U} = \frac{K}{2}\left(\cos\theta_{ijk} - \cos\theta_0\right)^2 . \tag{A.14}$$

The forces are therefore:

$$\begin{aligned} \mathbf{F_j} &= -\frac{\partial \mathcal{U}}{\partial \cos\theta_{ijk}}\frac{\partial \cos\theta_{ijk}}{\partial \mathbf{r_j}} \\ &= -\frac{K}{r_{ij}}\left(\cos\theta_{ijk} - \cos\theta_0\right)\left(\mathbf{\hat{r}_{ik}} - \cos\theta_{ijk}\mathbf{\hat{r}_{ij}}\right) , \end{aligned} \tag{A.15}$$

with $\mathbf{F_k}$ having an analogous form and $\mathbf{F_i}$ given by equation (A.9).

A.4 Restricted Bending Potential

The restricted bending (ReB) potential is a modification on the harmonic cosine angle potential which diverges at $\theta_{ijk} = 0, \pi$, ensuing angles cannot become reflex. The interaction between three particles with angle θ_{ijk} is given by:

$$\mathcal{U} = \frac{K}{2}\frac{\left(\cos\theta_{ijk} - \cos\theta_0\right)^2}{\sin^2\theta_{ijk}} . \tag{A.16}$$

The forces are therefore:

$$\begin{aligned}
\mathbf{F_j} &= -\frac{\partial \mathcal{U}}{\partial \cos\theta_{ijk}} \frac{\partial \cos\theta_{ijk}}{\partial \mathbf{r_j}} \\
&= -\frac{K}{r_{ij}\sin^4\theta_{ijk}} \left(\cos\theta_{ijk} - \cos\theta_0\right)\left(1 - \cos\theta_{ijk}\cos\theta_0\right)\left(\hat{\mathbf{r}}_{\mathbf{ik}} - \cos\theta_{ijk}\hat{\mathbf{r}}_{\mathbf{ij}}\right) \ , \qquad \text{(A.17)}
\end{aligned}$$

with $\mathbf{F_k}$ having an analogous form and $\mathbf{F_i}$ given by equation (A.9).

A.5 Keating Potential

The Keating potential combines the quartic stretching potential with a computationally efficient angle potential of the form:

$$\mathcal{U} = \frac{K}{2}\left(\mathbf{r_{ij}} \cdot \mathbf{r_{ik}} - r_0^2 \cos\theta_0\right)^2 \qquad \text{(A.18)}$$

for three particles with an angle given by $\mathbf{r_{ij}}$ and $\mathbf{r_{ik}}$. The forces are therefore:

$$\begin{aligned}
\mathbf{F_j} &= -\frac{\partial \mathcal{U}}{\partial \mathbf{r_j}} \\
&= -K\left(\mathbf{r_{ij}} \cdot \mathbf{r_{ik}} - r_0^2 \cos\theta_0\right)\mathbf{r_{ik}} \,, \qquad \text{(A.19)}
\end{aligned}$$

with $\mathbf{F_k}$ having an analogous form and $\mathbf{F_i}$ given by equation (A.9).

A.6 Proper Line Intersection

Some potential models have an additional term to prevent overlap of edges in a two-dimensional network, termed proper line intersection. This can be detected using standard computational geometry algorithms [**ORourke1998**]. The signed area of a triangle, A, is given by:

$$A\left(\mathbf{r_0}, \mathbf{r_1}, \mathbf{r_2}\right) = \frac{1}{2}\sum_{i=0}^{2}\left(x_i y_{i+1} - y_i x_{i+1}\right) \ . \qquad \text{(A.20)}$$

A point can then be designated "left" of a line segment if $A > 0$ and "right" otherwise. Overlap of two line segments can be detected if one point of one segment is "left" and the other point "right" with respect to the other segment, and no three points are collinear.

B | Additional Derivations and Formulae

This appendix outlines further derivations and formulae used throughout this thesis.

B.1 Ellipse Geometry

Section **??** considers the change in area when distorting a unit circle to an ellipse with the same circumference. An ellipse can be defined in terms of the major and minor axis radii, denoted a and b respectively. The distortion can then be described by the eccentricity, ξ, given by:

$$\xi = \left(1 - \frac{b^2}{a^2}\right)^{1/2} . \tag{B.1}$$

The circumference of an ellipse of given eccentricity, $C(\xi)$, can then be calculated from the complete elliptic integral of the second kind,

$$C(\xi) = 4a \int_0^{\pi/2} \left(1 - \xi^2 \sin^2\theta\right)^{1/2} \mathrm{d}\theta \,, \tag{B.2}$$

whilst the area is given more straightforwardly by

$$A = \pi ab \,. \tag{B.3}$$

The relative area between an ellipse and a unit circle for a given eccentricity is then

$$A/A^0 = ab \,, \tag{B.4}$$

where a,b satisfy $C(\xi) = 2\pi$.

B.2 Aboav-Weaire with aG

Section **??** considers the meaning of the Aboav-Weaire parameter for aG systems *i.e.* those containing just 5-, 6- and 7-rings. For these relatively constrained systems, α can be related specifically to the proportions of specific ring adjacencies. To derive this relationship, results are required from sections **??** and **??**.

The aG system has the node joint degree distribution

$$\mathbf{e} = \begin{array}{c} \begin{array}{ccc} 5 & 6 & 7 \end{array} \\ \begin{bmatrix} e_{55} & e_{56} & e_{57} \\ e_{65} & e_{66} & e_{67} \\ e_{75} & e_{76} & e_{77} \end{bmatrix} \end{array} \begin{array}{c} \\ 5 \\ 6 \\ 7 \end{array} . \tag{B.5}$$

Taking the Aboav-Weaire law, equation (1.20), and noting that $m_5 = \sum_k k e_{5k}/q_5$, leads to the relationship

$$\frac{5}{q_5}\left(5e_{55} + 6e_{66} + 7e_{57}\right) = \langle k \rangle^2 + \mu_2 + \langle k \rangle \left(1-\alpha\right)\left(5 - \langle k \rangle\right) , \tag{B.6}$$

to which several simplifications can be made. These arise from the constraints $\langle k \rangle = 6$ and $\sum_k e_{5k} = q_5$, which on substitution and rearrangement yield:

$$\begin{aligned} \frac{5}{q_5}\left(5e_{55} + 6\left(q_5 - e_{55} - e_{57}\right) + 7e_{57}\right) &= 36 + \mu_2 - 6\left(1-\alpha\right) \\ \frac{5}{q_5}\left(e_{57} - e_{55}\right) &= \mu_2 + 6\alpha \, . \end{aligned} \tag{B.7}$$

This can be further simplified by applying the relationships $q_5 = 5p_5/6$, $p_5 = \left(1-p_6\right)/2$, $\mu_2 = 1 - p_6$ and introducing the parameter $\chi^5_{75} = e_{57} - e_{55}$, to obtain:

$$\alpha = \frac{12\chi^5_{75} - \left(1-p_6\right)^2}{6\left(1-p_6\right)} \, . \tag{B.8}$$

This final relationship is the same as equation (**??**), which expresses the Aboav-Weaire parameter in terms of the difference between the 5-7 and 5-5 ring adjacencies.

B.3 Relating Aboav-Weaire to Assortativity

Section **??** provides a relationship between the assortativity and the Aboav-Weaire parameter, the derivation for which is detailed here. The assortativity is defined

$$r = \frac{\sum\limits_{jk} jk\left(e_{jk} - q_j q_k\right)}{\sum\limits_{k} k^2 q_k - \left(\sum\limits_{k} k q_k\right)^2}\,, \tag{B.9}$$

which can be rewritten by noting that $q_k = kp_k/\langle k\rangle$, in the form

$$r = \frac{\langle k\rangle^2 \sum\limits_{jk} jke_{jk} - \langle k^2\rangle^2}{\langle k\rangle\langle k^3\rangle - \langle k^2\rangle^2}\,. \tag{B.10}$$

The mean node degree about a node of degree j is given by $m_j = \frac{1}{q_j}\sum\limits_{k} e_{jk}$, which leads to the relationship

$$\sum_{jk} jke_{jk} = \sum_{j} jq_j m_j = \frac{1}{\langle k\rangle}\sum_{j} jp_j j m_j\,, \tag{B.11}$$

that contains within it the left hand component of the Aboav-Weaire law, equation (1.20). Substituting and simplifying gives:

$$\begin{aligned}
\sum_{jk} jke_{jk} &= \frac{1}{\langle k\rangle}\sum_{j} jp_j\left[\langle k\rangle^2 + \mu_2 + \langle k\rangle\left(1-\alpha\right)\left(j - \langle k\rangle\right)\right] && \text{(B.12)}\\
&= \frac{1}{\langle k\rangle}\left[\langle k\rangle\left(1-\alpha\right)\sum_{j} j^2 p_j + \left(\alpha\langle k\rangle^2 + \mu_2\right)\sum_{j} jp_j\right]\\
&= \langle k^2\rangle\left(1-\alpha\right) + \alpha\langle k\rangle^2 + \mu_2\\
&= -\alpha\mu_2 + \mu_2 + \langle k^2\rangle\,. && \text{(B.13)}
\end{aligned}$$

This allows equation (B.10) to be written

$$r = \frac{-\alpha\mu_2 + \mu_2\langle k\rangle^2 + \langle k^2\rangle\langle k\rangle^2 - \langle k^2\rangle^2}{\langle k\rangle\langle k^3\rangle - \langle k^2\rangle^2} \tag{B.14}$$

$$r = \frac{-\alpha\mu_2 - \mu_2^2\langle k\rangle^2}{\langle k\rangle\langle k^3\rangle - \langle k^2\rangle^2}$$

$$\alpha = -\frac{r\left(\langle k\rangle\langle k^3\rangle - \langle k^2\rangle^2\right)}{\mu_2\langle k\rangle^2} - \frac{\mu_2}{\langle k\rangle^2}\,, \tag{B.15}$$

which is the final form given in equation (**??**).

C | Analysis of Geopolitical Regions

This appendix outlines how network analysis can be performed on maps of geopolitical regions. The maps used as examples in this thesis are the communes of Switzerland (CH), the parishes and Westminster constituencies of Great Britain (GB) and the socio-economic regions of the EU and EFTA (including both current and candidate countries at the time of writing), termed NUTS [164–166]. These are displayed in figures **??** and C.2.

Geopolitical tilings can be thought of as consisting of tessellating administrative regions, where each administrative region on the map is defined by a boundary. Regions can be said to be neighbours if they share at least one point anywhere along the boundary. Vertices then form where three regions share a boundary and edges where two regions share a boundary. In analogue to materials, the size of an administrative region is then defined as the number of neighbours (equivalent to the number of vertices or edges), as can be seen in figure C.1a.

Analysis of these geopolitical networks is slightly complicated by the possible presence of defects. Defects arise when regions have $k < 3$ neighbours, either as a result of small imperfections in the boundary data or from legitimate region arrangements. For instance, if $k = 0$, the region is an island, if $k = 1$ a region is fully inscribed within another (usually indicative of a large urban area) and if $k = 2$ a region sits on a ring edge. Examples of these defects are given in figure C.1b. As these structures are primarily for illustrative purposes, these defects can be simply discounted for the purposed of the network analysis. A summary of the results from these geopolitical tilings is given in table C.1.

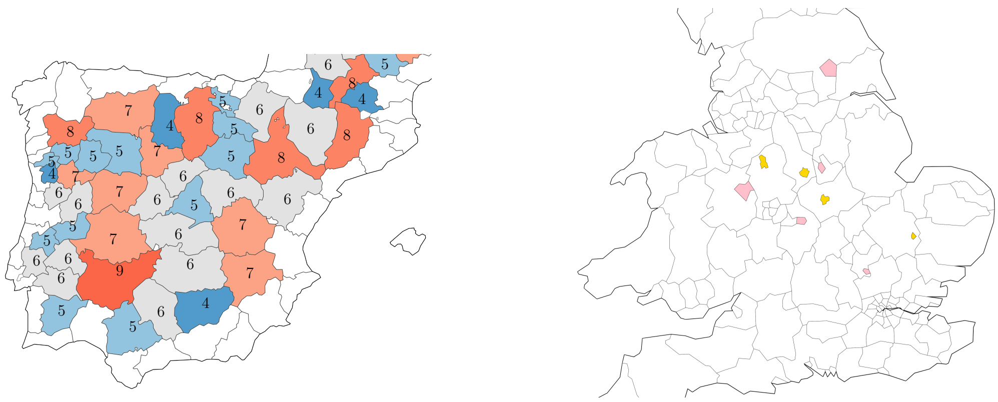

(a) (b)

Figure C.1: Panel (a) demonstrates how the number of neighbours of an administrative region defines the region size (as indicated by central numbers), in analogue with generic polygons. Panel(b) gives examples of the two defect types found in maps. Point defects (yellow) occur when a region is fully inscribed within another, and line defects (pink) when a region sits on the boundary between two others.

Table C.1: A network analysis of geopolitical results. The number of total and interior regions (without defects) are given for each map. The interior regions were then used to calculate the network properties.

Region	Total	Interior	$\langle k \rangle$	p_6	μ_2	r
CH communes	2379	2051	5.914	0.206	3.825	-0.151
GB parishes	11663	10778	6.005	0.241	3.028	-0.163
GB West. const.	654	455	5.930	0.251	3.019	-0.110
EU/EFTA NUTS 2	387	145	5.897	0.283	1.913	-0.215
EU/EFTA NUTS 3	1617	972	5.910	0.271	2.531	-0.161

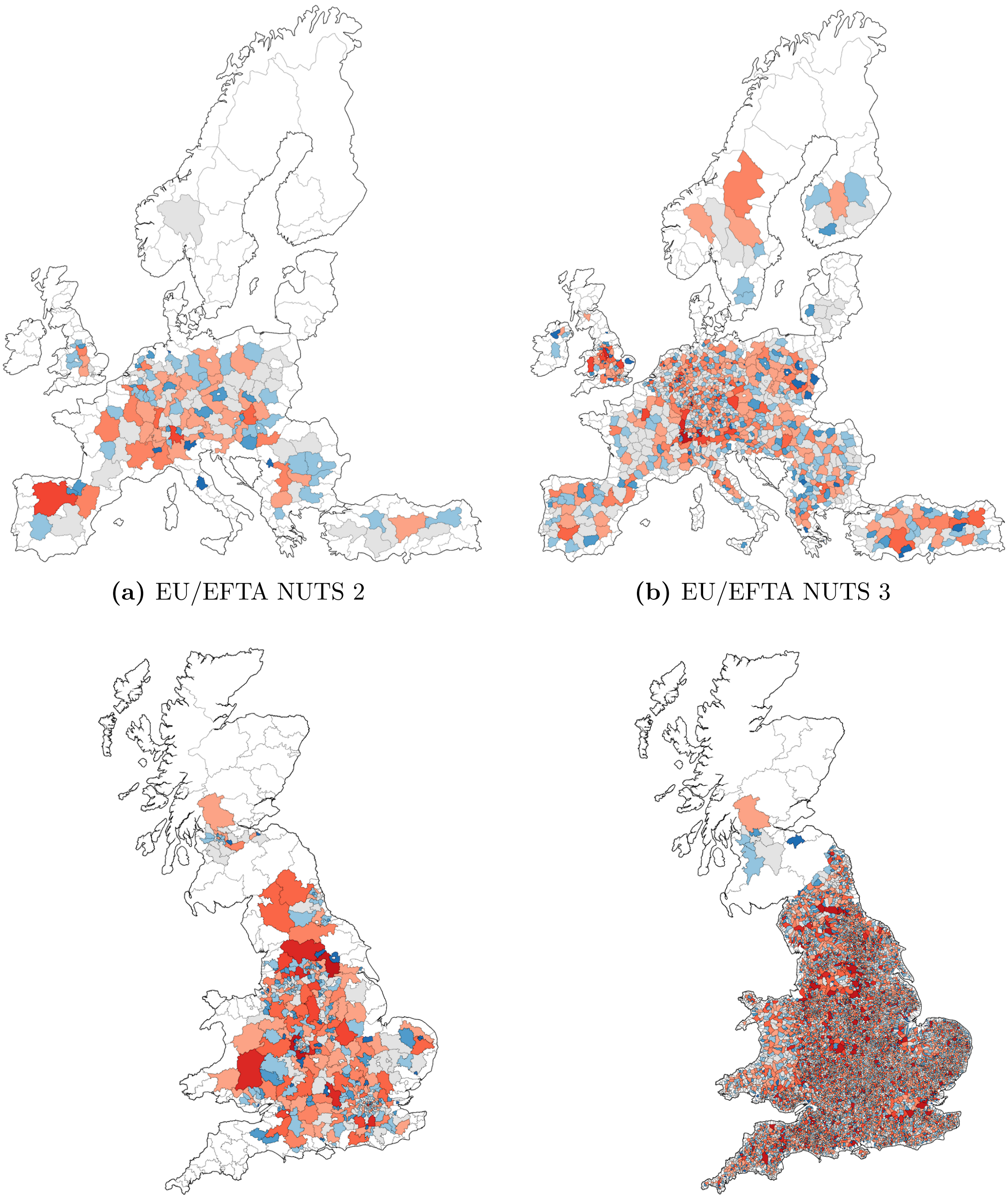

(a) EU/EFTA NUTS 2

(b) EU/EFTA NUTS 3

(c) GB Westminster constituencies

(d) GB parishes

Figure C.2: Geopolitical regions used for network analysis, in addition to the communes of Switzerland in figure **??**. Regions on sea frontiers are neglected, as are those completely surrounded by another region (shaded white).

References

[1] W H Zachariasen. “The Atomic Arrangement in Glass”. In: *J. Am. Chem. Soc.* 54.10 (1932), pp. 3841–3851.

[2] J. Kotakoski et al. “From point defects in graphene to two-dimensional amorphous carbon”. In: *Phys. Rev. Lett.* 106 (2011), p. 105505.

[3] Alex W. Robertson et al. “Spatial control of defect creation in graphene at the nanoscale”. In: *Nat. Commun.* 3 (2012), p. 1144.

[4] Pinshane Y Huang et al. “Direct Imaging of the a Two-Dimensional Silica Glass on Graphene”. In: *Nano Lett.* 12 (2012), pp. 1081–1086.

[5] Leonid Lichtenstein, Markus Heyde, and Hans Joachim Freund. “Atomic arrangement in two-dimensional silica: From crystalline to vitreous structures”. In: *J. Phys. Chem. C* 116 (2012), pp. 20426–20432.

[6] Shamil Shaikhutdinov and Hans-joachim Freund. “Metal-Supported Aluminosilicate Ultrathin Films as a Versatile Tool for Studying the Surface Chemistry of Zeolites”. In: *ChemPhysChem* 14 (2013), pp. 71–77.

[7] Adrián Leandro Lewandowski et al. “Atomic structure of a metal-supported two-dimensional germania film”. In: *Phys. Rev. B* 97 (2018), p. 115406.

[8] L Lewandowski et al. “From Crystalline to Amorphous Germania Bilayer Films at the Atomic Scale: Preparation and Characterization”. In: *Angew. Chem. Int. Ed.* 58 (2019), pp. 10903–10908.

[9] Panagiotis Trogadas, Thomas F Fuller, and Peter Strasser. “Carbon as catalyst and support for electrochemical energy conversion”. In: *Carbon N. Y.* 75 (2014), pp. 5–42.

[10] Yongfu Sun et al. “Ultrathin Two-Dimensional Inorganic Materials : New Opportunities for Solid State Nanochemistry”. In: *Acc. Chem. Res.* 48 (2015), pp. 3–12.

[11] Christin Büchner and Markus Heyde. “Two-dimensional silica opens new perspectives”. In: *Prog. Surf. Sci.* 92 (2017), pp. 341–374.

[12] Paul A Beck. “Annealing of cold worked metals”. In: *Adv. Phys.* 3.11 (1954), pp. 245–324.

[13] C G Dunn and E F Koch. “Comparison of Dislocation Densities of Primary and Secondary Recrystallization Grains of Si-Fe”. In: *Acta Metall.* 5 (1957), p. 548.

[14] A J Stone and D J Wales. “Theoretical Studies of Icosahedra C60 and Some Related Species”. In: *Chem. Phys. Lett.* 128.5,6 (1986), pp. 501–503.

[15] J. Shackelford and B. D. Brown. “The Lognormal Distribution in the Random Network Structure”. In: *J. Non. Cryst. Solids* 44 (1981), pp. 379–382.

[16] J Lemaitre et al. “Arrangement of cells in Voronoi tesselations of monosize packing of discs”. In: *Philos. Mag. B* 67.3 (1993), pp. 347–362.

[17] Leonid Lichtenstein et al. “The atomic structure of a metal-supported vitreous thin silica film”. In: *Angew. Chemie - Int. Ed.* 51 (2012), pp. 404–407.

[18] D A Aboav. “Arrangement of grains in a polycrystal”. In: *Metallography* 3 (1970), pp. 383–390.

[19] D. Weaire. “Some remarks on the arrangement of grains in a polycrystal”. In: *Metallography* 7 (1974), pp. 157–160.

[20] Torbjörn Björkman et al. “Defects in bilayer silica and graphene: Common trends in diverse hexagonal two-dimensional systems”. In: *Sci. Rep.* 3 (2013), p. 3482.

[21] Andrei Malashevich, Sohrab Ismail-Beigi, and Eric I. Altman. “Directing the structure of two-dimensional silica and silicates”. In: *J. Phys. Chem. C* 120 (2016), pp. 26770–26781.

[22] Mark Wilson et al. “Modeling vitreous silica bilayers”. In: *Phys. Rev. B* 87 (2013), p. 214108.

[23] Mark Wilson and Harry Jenkins. “Crystalline thin films of silica : modelling , structure and energetics”. In: *J. Phys. Condens. Matter* 30 (2018), p. 475401.

[24] Jin Zhang. “Phase-dependent mechanical properties of two-dimensional silica films: A molecular dynamics study”. In: *Comput. Mater. Sci.* 142 (2018), pp. 7–13.

[25] Franz Bamer, Firaz Ebrahem, and Bernd Markert. “Athermal mechanical analysis of Stone-Wales defects in two-dimensional silica”. In: *Comput. Mater. Sci.* 163 (2019), pp. 301–307.

[26] Projesh Kumar Roy and Andreas Heuer. “Ring Statistics in 2D Silica: Effective Temperatures in Equilibrium”. In: *Phys. Rev. Lett.* 122 (2019), p. 016104.

[27] Nina F. Richter et al. “Characterization of Phonon Vibrations of Silica Bilayer Films”. In: *J. Phys. Chem. C* 123 (2019), pp. 7110–7117.

[28] Projesh Kumar Roy, Markus Heyde, and Andreas Heuer. “Modelling the atomic arrangement of amorphous 2D silica: a network analysis”. In: *Phys. Chem. Chem. Phys.* 20 (2018), pp. 14725–14739.

[29] Avishek Kumar et al. “Ring statistics of silica bilayers”. In: *J. Phys. Condens. Matter* 26 (2014), p. 395401.

[30] D. A. Aboav. “The arrangement of cells in a net. I”. In: *Metallography* 13 (1980), pp. 43–58.

[31] B. N. Boots. “Comments on "Aboav’s Rule" for the Arrangement of Cells in a Network”. In: *Metallography* 17 (1984), pp. 411–418.

[32] J. C. Earnshaw and D. J. Robinson. “Topological correlations in colloidal aggregation”. In: *Phys. Rev. Lett.* 72.23 (1994), p. 3682.

[33] C Allain and L Limat. “Regular Patterns of Cracks Formed by Directional Drying of a Collodial Suspension”. In: *Phys. Rev. Lett.* 74.15 (1995), p. 2981.

[34] A Moncho-Jorda, F Martinez-Lopez, and R Hidalgo-Alvarez. “Simulations of aggregation in 2D . A study of kinetics , structure and topological properties”. In: *Physica A* 282 (2000), pp. 50–64.

[35] Marc Durand et al. “Statistical mechanics of two-dimensional shuffled foams: Prediction of the correlation between geometry and topology”. In: *Phys. Rev. Lett.* 107 (2011), p. 168304.

[36] Mingming Tong et al. “Geometry and Topology of Two-Dimensional Dry Foams : Computer Simulation and Experimental Characterization”. In: *Langmuir* 33 (2017), pp. 3839–3846.

[37] Lucas Goehring and Stephen W Morris. “Cracking mud, freezing dirt, and breaking rocks”. In: *Phys. Today* 67.11 (2014), p. 39.

[38] D Brutin et al. “Pattern formation in drying drops of blood”. In: *J. Fluid Mech.* 667 (2011), pp. 85–95.

[39] Franziska Glassmeier and Graham Feingold. “Network approach to patterns in stratocumulus clouds”. In: *PNAS* 114.40 (2017), pp. 10578–10583.

[40] Michel C Milinkovitch et al. “Crocodile Head Scales Are Not Developmental Units But Emerge From Physical Cracking”. In: *Science (80-.).* 339 (2019), pp. 78–81.

[41] G. Le Caër and R. Delannay. “The administrative divisions of mainland France as 2D random cellular structures”. In: *J. Phys. Fr.* 3 (1993), p. 1777.

[42] G Schliecker and S Klapp. “Why are the equilibrium properties of two-dimensional random cellular structures so similar?” In: *Europhys. Lett.* 48.2 (1999), pp. 122–128.

[43] William T. Gibson et al. “Control of the mitotic cleavage plane by local epithelial topology”. In: *Cell* 144 (2011), pp. 427–438.

[44] M Kokalj Ladan, P Ziherl, and A Šiber. “Topology of dividing planar tilings : Mitosis and order in epithelial tissues”. In: *Phys. Rev. E* 100 (2019), p. 012410.

[45] D. Weaire and N. Rivier. “Soap, cells and statistics-random patterns in two dimensions”. In: *Contemp. Phys.* 50.1 (2009), pp. 199–239.

[46] J C Flores. “Mean-field crack networks on desiccated films and their applications : Girl with a Pearl Earring”. In: *Soft Matter* 13 (2017), pp. 1352–1356.

[47] Steven H Strogatz. “Exploring complex networks”. In: *Nature* 410 (2001), p. 268.

[48] S Boccaletti et al. “Complex networks : Structure and dynamics”. In: *Phys. Rep.* 424 (2006), pp. 175–308.

[49] Albert-László Barabási. “The network takeover”. In: *Nat. Phys.* 8 (2012), pp. 14–16.

[50] Alice L. Thorneywork et al. “Two-Dimensional Melting of Colloidal Hard Spheres”. In: *Phys. Rev. Lett.* 118 (2017), p. 158001.

[51] Andrew B Cairns et al. “Design of crystal-like aperiodic solids with selective disorder–phonon coupling”. In: *Nat. Commun.* 7 (2016), p. 10445.

[52] Albert-László Barabási and Márton Pósfai. *Network science.* Cambridge: Cambridge University Press, 2016.

[53] Xianglong Yuan and A N Cormack. "Efficient algorithm for primitive ring statistics in topological networks". In: *Comput. Mater. Sci.* 24 (2002), pp. 343–360.

[54] D. A. Aboav. "The Arrangement of Cells in a Net. III". In: *Metallography* 17 (1984), pp. 383–396.

[55] E Ressouche et al. "Magnetic Frustration in an Iron-Based Cairo Pentagonal Lattice". In: *Phys. Rev. Lett.* 103 (2009), p. 267204.

[56] P W Fowler et al. "Energetics of Fullerenes with Four-Membered Rings". In: *J Phys Chem* 100 (1996), pp. 6984–6991.

[57] A. Gervois, J. P. Troadec, and J. Lemaitre. "Universal properties of Voronoi tessellations of hard discs". In: *J. Phys. A* 25 (1992), pp. 6169–6177.

[58] G. Le Caër and R. Delannay. "Correlations in Topological Models of 2d Random Cellular Structures". In: *J. Phys. A* 26 (1993), pp. 3931–3954.

[59] P Cerisier, S Rahal, and N Rivier. "Topological correlations in Benard-Marangoni convective structures". In: *Phys. Rev. E* 54.5 (1996), pp. 5086–5094.

[60] Matthew P. Miklius and Sascha Hilgenfeldt. "Analytical results for size-topology correlations in 2D disk and cellular packings". In: *Phys. Rev. Lett.* 108 (2012), p. 015502.

[61] N Rivier, D Weaire, and R Romer. "Tetrahedrally Bonded Random Networks Without Odd Rings". In: *J. Non. Cryst. Solids* 105 (1988), pp. 287–291.

[62] F. T. Lewis. "The correlation between cell division and the shapes and sizes of prismatic cell in the epidermis of cucumis". In: *Anat. Rec.* 38.3 (1928), pp. 341–376.

[63] M. A. Fortes. "Applicability of the Lewis and Aboav-Weaire laws to 2D and 3D cellular structures based on Poisson partitions". In: *J. Phys. A* 28 (1995), pp. 1055–1068.

[64] Sangwoo Kim, Muyun Cai, and Sascha Hilgenfeldt. "Lewis' law revisited: the role of anisotropy in size-topology correlations". In: *New J. Phys.* 16 (2014), p. 015024.

[65] S. N. Chiu. "Aboav-Weaire's and Lewis' laws - A review". In: *Mater. Charact.* 34 (1995), pp. 149–165.

[66] Renaud Delannay and Gérard Le Caër. "Topological characteristics of 2D cellular structures generated by fragmentation". In: *Phys. Rev. Lett.* 73.11 (1994), pp. 1553–1556.

[67] S Le Roux and F Rezai-Aria. "Topological and metric properties of microscopic crack patterns : application to thermal fatigue of high temperature". In: *J. Phys. D* 46 (2013), p. 295301.

[68] David A Noever. "Statistics of emulsion lattices". In: *Colloids and Surfaces* 62 (1992), pp. 243–247.

[69] J. C. M. Mombach, R. M. C. de Almeida, and J. R. Iglesias. "Two-cell correlations in biological tissues". In: *Phys. Rev. E* 47.5 (1993), pp. 3712–3717.

[70] P Pedro et al. "Polygonal terrains on Mars : A contribution to their geometric and topological characterization". In: *Planet. Space Sci.* 56 (2008), pp. 1919–1924.

[71] David P Landau and Kurt Binder. *A Guide to Monte Carlo Simulations in Statistical Physics*. 4th ed. Cambridge University Press, 2014.

[72] David J Wales and Harold A Scheraga. “Global Optimization of Clusters, Crystals, and Biomolecules”. In: *Science (80-.).* 285 (1999), pp. 1368–1372.

[73] Andrea C Levi and Miroslav Kotrla. “Theory and simulation of crystal growth”. In: *J. Phys. Condens. Matter* 9 (1997), p. 299.

[74] C Ratsch and J A Venables. “Nucleation Theory and the Early Stages of Thin Film Growth”. In: *J. Vac. Sci. Technol. A* 21 (2003), S96.

[75] Wlater Kob. “Computer simulations of supercooled liquids and glasses”. In: *J. Phys. Condens. Matter* 11 (1999), R85.

[76] Pablo Jensen. “Growth of nanostructures by cluster deposition: Experiments and simple models”. In: *Rev. Mod. Phys.* 71.5 (1999), pp. 1695–1735.

[77] Daan Frenkel and Berend Smit. *Understanding Molecular Simulation: from Algorithms to Applications*. 2nd ed. Academic Press, 2002.

[78] M P Allen and D J Tildesley. *Computer simulation of liquids*. 2nd ed. Oxford Science Publications, 2017.

[79] Steve Brooks et al. *Handbook of Markov Chain Monte Carlo*. CRC Press, 2011.

[80] N Metropolis et al. “Equation of State Calculations by Fast Computing Machines”. In: *J. Chem. Phys.* 21.6 (1953), pp. 1087–1092.

[81] Vasilios I Manousiouthakis and Michael W Deem. “Strict detailed balance is unnecessary in Monte Carlo simulation”. In: *J. Chem. Phys.* 110 (1999), p. 2753.

[82] Hidemaro Suwa and Synge Todo. “Markov Chain Monte Carlo Method without Detailed Balance”. In: *Phys. Rev. Lett.* 105 (2010), p. 120603.

[83] Manon Michel, Sebastian C Kapfer, and Werner Krauth. “Generalized event-chain Monte Carlo:” in: *J. Chem. Phys.* 140 (2014), p. 054116.

[84] G M Torrie and J P Valleau. “Nonphysical Sampling Distributions in Monte Carlo Free-Energy Estimation: Umbrella Sampling”. In: *J. Comput. Phys.* 23 (1977), pp. 187–199.

[85] David J Earl and Michael W Deem. “Parallel tempering: Theory, applications, and new perspectives”. In: *Phys. Chem. Chem. Phys.* 7 (2005), pp. 3910–3916.

[86] Bernd Hartke. “Global Geometry Optimization of Clusters Using Genetic Algorithms”. In: *J. Phys. Chem.* 97 (1993), pp. 9973–9976.

[87] J A Niesse and Howard R Mayne. “Global geometry optimization of atomic clusters using a modified genetic algorithm in space-fixed coordinates”. In: *J. Chem. Phys.* 105 (1996), p. 4700.

[88] David J Wales and Jonathan P K Doye. “Global Optimization by Basin-Hopping and the Lowest Energy Structures of Lennard-Jones Clusters Containing up to 110 Atoms”. In: *J. Phys. Chem. A* 101 (1997), pp. 5111–5116.

[89] S . Kirkpatrick, C . D . Gelatt Jr., and M . P . Vecchi. “Optimization by Simulated Annealing”. In: *Science (80-.).* 220.4598 (1983), pp. 671–680.

[90] Darrall Henderson, Sheldon H Jacobson, and Alan W Johnson. “The Theory and Practice of Simulated Annealing”. In: *Handb. Metaheuristics.* Ed. by Fred Glover and Gary A Kochenberger. Boston, MA: Springer US, 2003, pp. 287–319.

[91] F Wooten, K Winer, and D Weaire. “Computer Generation of Structural Models of Amorphous Si and Ge”. In: *Phys. Rev. Lett.* 54.13 (1985), pp. 1392–1395.

[92] M M J Treacy and K B Borisenko. “The Local Structure of Amorphous Silicon”. In: *Science (80-.).* 335 (2012), pp. 950–953.

[93] Yuhai Tu et al. “Properties of a Continuous-Random-Network Model for Amorphous Systems”. In: *Phys. Rev. Lett.* 81.22 (1998), pp. 4899–4902.

[94] B R Djordjevic, M F Thorpe, and F Wooten. “Computer model of tetrahedral amorphous diamond”. In: *Phys. Rev. B* 52.8 (1995), pp. 5685–5690.

[95] Normand Mousseau and G T Barkema. “Binary continuous random networks”. In: *J. Phys. Condens. Matter* 16 (2004), S5183–S5190. arXiv: `0408705 [cond-mat]`.

[96] E M Huisman, C Storm, and G T Barkema. “Monte Carlo study of multiply crosslinked semiflexible polymer networks”. In: *Phys. Rev. E* 78 (2008), p. 051801.

[97] C P Broedersz and F C Mackintosh. “Modeling semiflexible polymer networks”. In: *Rev. Mod. Phys.* 86 (2014), pp. 995–1036.

[98] Sandeep K Jain and Gerard T Barkema. “Rupture of amorphous graphene via void formation”. In: *PCCP* 20 (2018), pp. 16966–16972.

[99] Avishek Kumar, Mark Wilson, and M F Thorpe. “Amorphous graphene: a realization of Zachariasen’s glass”. In: *J. Phys. Condens. Matter* 24 (2012), p. 485003.

[100] P. N. Keating. “Effect of invariance requirements on the elastic strain energy of crystals with application to the diamond structure”. In: *Phys. Rev.* 145.2 (1966), pp. 637–645.

[101] G. Barkema and Normand Mousseau. “High-quality continuous random networks”. In: *Phys. Rev. B* 62.8 (2000), pp. 4985–4990.

[102] D A Drabold. “Topics in the theory of amorphous materials”. In: *Eur Phys J B* 68 (2009), pp. 1–21.

[103] S. von Alfthan, A. Kuronen, and K. Kaski. “Realistic models of amorphous silica: A comparative study of different potentials”. In: *Phys. Rev. B* 68 (2003), p. 073203.

[104] Monica Bulacu et al. “Improved Angle Potentials for Coarse-Grained Molecular Dynamics Simulations”. In: *J. Chem. Theory Comput.* 9 (2013), pp. 3282–3292.

[105] Jorge Nocedal and Stephen J Wright. *Numerical Optimization.* 2nd ed. Springer, 2006.

[106] Normand Mousseau and G. T. Barkema. “Fast bond-transposition algorithms for generating covalent amorphous structures”. In: *Curr. Opin. Solid State Mater. Sci.* 5 (2001), pp. 497–502.

[107] Masaharu Isobe. “Hard sphere simulation in statistical physics - methodologies and applications”. In: *Mol. Simul.* 42.16 (2016), pp. 1317–1329.

[108] Etienne P Bernard, Werner Krauth, and David B Wilson. “Event-chain Monte Carlo algorithms for hard-sphere systems”. In: *Phys. Rev. E* 80 (2009), p. 056704.

[109] Joshua A Anderson et al. “Massively parallel Monte Carlo for many-particle simulations on GPUs”. In: *J. Comput. Phys.* 254 (2013), pp. 27–38.

[110] Masaharu Isobe and Werner Krauth. “Hard-sphere melting and crystallization with event-chain Monte Carlo”. In: *J. Chem. Phys.* 143 (2015), p. 084509.

[111] B Widom. “Random Sequential Addition of Hard Spheres to a Volume”. In: *J Chem Phys* 44 (1966), p. 3888.

[112] T S Grigera and G Parisi. “Fast Monte Carlo algorithm for supercooled soft spheres”. In: *Phys. Rev. E* 63 (2001), 045102(R).

[113] Andrea Ninarello, Ludovic Berthier, and Daniele Coslovich. “Models and Algorithms for the Next Generation of Glass Transition Studies”. In: *Phys. Rev. X* 7 (2017), p. 021039.

[114] A Okabe, B Boots, and K Sugihara. *Spatial Tessellations: Concepts and Applications of Voronoi Diagrams.* Wiley, 1992.

[115] Anne Poupon. “Voronoi and Voronoi-related tessellations in studies of protein structure and interaction”. In: *Curr. Opin. Struct. Biol.* 14 (2004), pp. 233–241.

[116] B. J. Gellatly and J. L. Finney. “Characterisation of Models of Multicomponent Amorphous Metals: the Radical Alternative to the Voronoi Polyhedron”. In: *J. Non. Cryst. Solids* 50 (1982), pp. 313–329.

[117] F Aurenhammer. “Power diagrams: properties, algorithms and applications”. In: *SIAM J Comput* 16.1 (1987), pp. 78–96.

[118] FM Richards. “The Interpretation of Protein Structures : Total Volume, Group Volume Distributions and Packing Density”. In: *J Mol Biol* 82 (1974), pp. 1–14.

[119] B N Boots. “The Spatial Arrangement of Random Voronoi Polygons”. In: *Comput. Geosci.* 9.3 (1983), pp. 351–365.

[120] Masaharu Tanemura. “Statistical Distributions of Poisson Voronoi Cells in Two and Three Dimensions”. In: *Forma* 18 (2003), pp. 221–247.

[121] Chris H Rycroft. “VORO++ : A three-dimensional Voronoi cell library in C ++”. In: *Chaos* 19 (2009), p. 041111.

[122] D. Löffler et al. “Growth and structure of crystalline silica sheet on Ru(0001)”. In: *Phys. Rev. Lett.* 105 (2010), p. 146104.

[123] Leonid Lichtenstein, Markus Heyde, and Hans Joachim Freund. “Crystalline-vitreous interface in two dimensional silica”. In: *Phys. Rev. Lett.* 109 (2012), p. 106101.

[124] Mahdi Sadjadi et al. “Refining glass structure in two dimensions”. In: *Phys. Rev. B* 96 (2017), 201405(R).

[125] James F. Shackelford. “Triangle rafts - extended Zachariasen schematics for structure modeling”. In: *J. Non. Cryst. Solids* 49 (1982), pp. 19–28.

[126] Christin Büchner et al. “Building block analysis of 2D amorphous networks reveals medium range correlation”. In: *J. Non. Cryst. Solids* 435 (2016), pp. 40–47.

[127] Louis Theran et al. “Anchored boundary conditions for locally isostatic networks”. In: *Phys. Rev. E* 92 (2015), p. 053306.

[128] P. Tangney and S. Scandolo. “An ab initio parametrized interatomic force field for silica”. In: *J. Chem. Phys.* 117 (2002), pp. 8898–8904.

[129] I. Zsoldos and A. Szasz. “Appearance of collectivity in two-dimensional cellular structures”. In: *Comput. Mater. Sci.* 15 (1999), pp. 441–448.

[130] Mahdi Sadjadi and M. F. Thorpe. “Ring correlations in random networks”. In: *Phys. Rev. E* 94 (2016), p. 062304.

[131] S R Broadbent and J M Hammersley. “Percolation processes I. Crystals and Mazes”. In: *Proc. Camb. Phil. Soc.Phil. Soc.* 53 (1956), pp. 629–641.

[132] Duncan S Callaway et al. “Network Robustness and Fragility : Percolation on Random Graphs”. In: *Phys. Rev. Lett.* 85.25 (2000), p. 5468.

[133] Dietrich Stauffer and Amnon Aharony. *Introduction to percolation theory.* 2nd ed. 2014.

[134] M F Sykes and J W Essam. “Exact Critical Percolation Probabilities for Site and Bond Problems in Two Dimensions”. In: *J. Math. Phys.* 5.8 (1964), p. 1117.

[135] Scott Kirkpatrick. “Percolation and Conduction”. In: *Rev. Mod. Phys.* 45.4 (1973), p. 574.

[136] H L Frisch, J M Hammersley, and D J A Welsh. “Monte Carlo Estimates of Percolation Probabilities for Various Lattices”. In: *Phys. Rev.* 126.3 (1962), pp. 949–951.

[137] B Y P Dean and N F Bird. “Monte Carlo estimates of critical percolation probabilities”. In: *Proc. Camb. Phil. Soc.* 63 (1967), p. 477.

[138] M E J Newman. “Mixing patterns in networks”. In: *Phys. Rev. E* 67 (2003), p. 026126.

[139] Di Zhou et al. “Assortativity decreases the robustness of interdependent networks”. In: *Phys. Rev. E* 86 (2012), p. 066103.

[140] C Schmeltzer et al. “Percolation of spatially constrained Erdos-Renyi networks with degree correlations”. In: *Phys. Rev. E* 89 (2014), p. 012116.

[141] V Kapko, D A Drabold, and M F Thorpe. “Electronic structure of a realistic model of amorphous graphene”. In: *Phys. Status Solidi* 247.5 (2010), pp. 1197–1200.

[142] Taishan Zhu and Elif Ertekin. “Phonons, Localization, and Thermal Conductivity of Diamond Nanothreads and Amorphous Graphene”. In: *Nano Lett.* 16 (2016), pp. 4763–4772.

[143] Franz Bamer, Firaz Ebrahem, and Bernd Markert. “Elementary plastic events in a Zachariasen glass under shear and pressure”. In: *Materialia* 9 (2020), p. 100556.

[144] Firaz Ebrahem, Franz Bamer, and Bernd Markert. “Vitreous 2D silica under tension : From brittle to ductile behaviour”. In: *Mater. Sci. Eng. A* 780 (2020), p. 139189.

[145] Oliver Whitaker. “Modelling of complex ring networks in two- and three-dimensions”. PhD thesis. University of Oxford, 2019.

[146] Xiaolei Ma, Janna Lowensohn, and Justin C Burton. "Universal scaling of polygonal desiccation crack patterns". In: *Phys. Rev. E* 99 (2019), p. 012802.

[147] Hisao Honda. "Description of cellular patterns by Dirichlet domains: The two-dimensional case". In: *J. Theor. Biol.* 72 (1978), pp. 523–543.

[148] Ross Carter et al. "Pavement cells and the topology puzzle". In: *Development* 144 (2017), pp. 4386–4397.

[149] Sangwoo Kim et al. "Hexagonal Patterning of the Insect Compound Eye : Facet Area Variatio , Defects, and Disorder". In: *Biophys. J.* 111 (2016), pp. 2735–2746.

[150] C. J. Lambert and D. L. Weaire. "Theory of the arrangement of cells in a network". In: *Metallography* 14.4 (1981), pp. 307–318.

[151] Susmit Kumar, Stewart K. Kurtz, and Denis Weaire. "Average number of sides for the neighbours in a Poisson-Voronoi tesselation". In: *Philos. Mag. B* 69.3 (1994), pp. 431–435.

[152] M. Blanc and A. Mocellin. "Grain coordination in plane sections of polycrystals". In: *Acta Metall.* 27 (1979), pp. 1231–1237.

[153] N. Rivier. "Statistical crystallography structure of random cellular networks". In: *Philos. Mag. B* 52.3 (1985), pp. 795–819.

[154] Michael A. Peshkin, Katherine J. Strandburg, and Nicolas Rivier. "Entropic predictions for cellular networks". In: *Phys. Rev. Lett.* 67.13 (1991), pp. 1803–1806.

[155] S N Chiu. "Mean-Value Formulae for the Neighbourhood of the Typical Cell of a Random Tessellation". In: *Adv. Appl. Probab.* 26 (1994), pp. 565–576.

[156] J K Mason, R Ehrenborg, and E A Lazar. "A geometric formulation of the law of Aboav – Weaire in two and three dimensions". In: *J. Phys. A* 45 (2012), p. 065001.

[157] H. J. Hilhorst. "Planar Voronoi cells: The violation of Aboav's law explained". In: *J. Phys. A* 39 (2006), pp. 7227–7243.

[158] M. E.J. Newman. "Assortative Mixing in Networks". In: *Phys. Rev. Lett.* 89.20 (2002), pp. 1–4.

[159] Rogier Noldus and Piet Van Mieghem. "Assortativity in complex networks". In: *J. Complex Networks* 3 (2015), pp. 507–542.

[160] Alexandros Chremos and Philip J. Camp. "Neighbor network in a polydisperse hard-disk fluid: Degree distribution and assortativity". In: *Phys. Rev. E* 76 (2007), p. 056108.

[161] Nelly Litvak and Remco van der Hofstad. "Uncovering disassortativity in large scale-free networks". In: *Phys. Rev. E* 87 (2013), p. 022801.

[162] J M Greneche and J M D Coey. "The topologically-disordered square lattice". In: *J. Phys. Fr.* 51 (1990), pp. 231–242.

[163] Franz R Eder et al. "A journey from order to disorder - atom by atom transformation from graphene to a 2D carbon glass". In: *Sci. Rep.* 4 (2014), p. 4060.

[164] Ordnance Survey. *Boundary-Line Data © Crown copyright and database right 2018*. 2018.

[165] Federal Office of Topography. *swissBOUNDARIES3D*. 2019.

[166] Eurostat. *NUTS Geodata © EuroGeographics for the administrative boundaries.* 2016.

[167] Etienne P Bernard and Werner Krauth. “Two-Step Melting in Two Dimensions : First-Order Liquid-Hexatic Transition”. In: *Phys. Rev. Lett.* 107 (2011), p. 155704.

[168] Andrew H Marcus and Stuart A Rice. “Phase transitions in a confined quasi-two-dimensional colloid suspension”. In: *Phys. Rev. E* 55.1 (1997), p. 637.

[169] Han-Rui Tian et al. “An Unconventional Hydrofullerene C66H4 with Symmetric Heptagons Retrieved in Low-Pressure Combustion”. In: *J. Am. Chem. Soc.* 141 (2019), pp. 6651–6657.

[170] Runnan Guan et al. “Stable C92(26) and C92(38) as Well as Unstable C92(50) and C92(23) Isolated-Pentagon-Rule Isomers As Revealed by Chlorination of C92 Fullerene”. In: *Inorg. Chem.* 58 (2019), pp. 5393–5396.

[171] Victor A Brotsman, Daria V Ignateva, and Sergey I Troyanov. “Chlorination-promoted Transformation of Isolated Pentagon Rule C78 into Fused-pentagons- and Heptagons-containing Fullerenes”. In: *Chem Asian J* 12 (2017), pp. 2379–2382.

[172] Victor A Brotsman et al. “Rebuilding C60 : Chlorination-Promoted Transformations of the Buckminsterfullerene into Pentagon-Fused C60 Derivatives”. In: *Inorg. Chem.* 57 (2018), pp. 8325–8331.

[173] Daishi Fujita et al. “Self-assembly of tetravalent Goldberg polyhedra from 144 small components”. In: *Nature* 540 (2016), pp. 563–566.

[174] Zhi Wang et al. “Assembly of silver Trigons into a buckyball-like Ag180 nanocage”. In: *PNAS* 114.46 (2017), pp. 12132–12137.

[175] A E Roth, C D Jones, and D J Durian. “Coarsening of a two-dimensional foam on a dome”. In: *Phys. Rev. E* 86 (2012), p. 021402.

[176] P N Pusey and W Van Megen. “Phase behaviour of concentrated suspensions of nearly hard colloidal spheres”. In: *Nature* 320 (1986), p. 340.

[177] Alice L Thorneywork et al. “Radial distribution functions in a two-dimensional binary colloidal hard sphere system”. In: *J. Chem. Phys.* 140 (2014), p. 161106.

[178] Alice L Thorneywork et al. “Structure factors in a two-dimensional binary colloidal hard sphere system”. In: *Mol. Phys.* 116 (2018), pp. 3245–3257.

[179] R Roth, R Evans, and A A Louis. “Theory of asymmetric nonadditive binary hard-sphere mixtures”. In: *Phys. Rev. E* 64 (2001), p. 051202.

[180] R Y Yang, R P Zou, and A B Yu. “Voronoi tessellation of the packing of fine uniform spheres”. In: *Phys. Rev. E* 65 (2002), 041302 Voronoi.

[181] VS Kumar and V Kumaran. “Voronoi neighbor statistics of hard-disks and hard-spheres”. In: *J Chem Phys* 123 (2005), p. 074502.

[182] A Jaster. “Computer simulations of the two-dimensional melting transition using hard disks”. In: *Phys. Rev. E* 59.3 (1999), pp. 2594–2602.

[183] Sander Pronk and Daan Frenkel. “Melting of polydisperse hard disks”. In: *Phys. Rev. E* 69 (2004), p. 066123.

[184] Sebastian C Kapfer and Werner Krauth. “Two-Dimensional Melting : From Liquid-Hexatic Coexistence to Continuous Transitions”. In: *Phys. Rev. Lett.* 114 (2015), p. 035702.

[185] Alice L Thorneywork. “Structure and dynamics of two-dimensional colloidal hard spheres”. PhD thesis. University of Oxford, 2015.

[186] Q Weikai, A P Gantapara, and Marjolein Dijkstra. “Two-stage melting induced by dislocations and grain boundaries in monolayers of hard spheres”. In: *Soft Matter* 10.30 (2014), p. 5449.

[187] Y Peng et al. “Short-time self-diffusion of nearly hard spheres at an oil–water interface”. In: *J Fluid Mech* 618 (2009), pp. 243–261.

[188] N Vogel et al. “Direct visualization of the interfacial position of colloidal particles and their assemblies†”. In: *Nanoscale* 6 (2014), pp. 6879–6885.

[189] Elisa Tamborini, C Patrick Royall, and Pietro Cicuta. “Correlation between crystalline order and vitrification in colloidal monolayers”. In: *J. Phys. Condens. Matter* 27 (2015), p. 194124.

[190] H Imai, I Masao, and K Murota. “Voronoi Diagram in the Laguerre Geometry and its Applications”. In: *SIAM J* 14.1 (1985), pp. 93–105.

[191] N Rivier. “Geometry and Fluctuations of Surfaces”. In: *J. Phys. Colloq.* 51 (1990), pp. 309–317.

[192] P Bhattacharyya and B K Chakrabarti. “The mean distance to the nth neighbour in a uniform distribution of random points: an application of probability theory”. In: *Eur. J. Phys.* 29 (2008), p. 639.

[193] L Oger et al. “Comparison of two representations of a random cut of identical sphere packing”. In: *Eur. Phys. J. B* 14 (2000), pp. 403–406.

[194] Annie Gervois, Luc Oger, and Jean-Paul Troadec. “Random cuts in binary mixtures of spheres”. In: *Phys. Rev. E* 70 (2004), p. 031112.

[195] U Hahn and U Lorz. “Stereological analysis of the spatial Poisson-Voronoi tessellation”. In: *J. Microsc.* 175.3 (1994), pp. 176–185.

[196] Simone Falco et al. “Generation of 3D polycrystalline microstructures with a conditioned Laguerre-Voronoi tessellation technique”. In: *Comput. Mater. Sci.* 136 (2017), pp. 20–28.

[197] Dorian Depriester and Régis Kubler. “Radical Voronoï tessellation from random pack of polydisperse spheres Prediction of the cells’ size distribution”. In: *Comput. Des.* 107 (2019), pp. 37–49.

[198] Matthew O Blunt et al. “Random Tiling and Topological Defects in a Two-Dimensional Molecular Network”. In: *Science (80-.).* 322 (2008), pp. 1077–1081.

[199] P W Anderson. “RESONATING VALENCE BONDS" A NEW KIND OF INSULATOR?” In: *Mat. Res. Bull.* 8 (1973), pp. 153–160.

[200] Philip J Camp, Amparo Fuertes, and J P Attfield. “Subextensive Entropies and Open Order in Perovskite Oxynitrides”. In: *J Am Chem Soc* 134 (2012), pp. 6762–6766.

[201] R Comes, M Lambert, and A Guinier. "THE CHAIN STHUCTURE OF BaT1O3 AND KNbO3". In: *Solid State Commun.* 6 (1968), pp. 715–719.

[202] G Algara-Siller et al. "Square ice in graphene nanocapillaries". In: *Nature* 519 (2015), p. 443.

[203] YinBo Zhu, FengChao Wang, and HengAn Wu. "Structural and dynamic characteristics in monolayer square ice". In: *J. Chem. Phys.* 147 (2017), p. 044706.

[204] Simon J Hibble et al. "Structures of Pd (CN)2 and Pt (CN)2: Intrinsically Nanocrystalline Materials?" In: *Inorg. Chem.* 50 (2011), pp. 104–113.

[205] Qing-Na Zheng et al. "Adaptive Reorganization of 2D Molecular Nanoporous Network Induced by Coadsorbed Guest Molecule". In: *Langmuir* 30 (2014), pp. 3034–3040.

[206] Lars Postulka et al. "Spin Frustration in an Organic Radical Ion Salt Based on a Kagome-Coupled Chain Structure". In: *J. Am. Chem. Soc.* 138 (2016), pp. 10738–10741.

[207] Ting Chen et al. "2D Hexagonal Tilings Based on Triangular and Hexagonal Structural Units in the Self-Assembly of Thiacalix[4]arene Tetrasulfonate on an Au(111) Surface". In: *Chem Asian J* 6 (2011), pp. 1811–1816.

[208] Austin D Griffith and Robert S Hoy. "Densest versus jammed packings of two-dimensional bent-core trimers". In: *Phys. Rev. E* 98 (2018), p. 042910.

[209] Jose I Urgel et al. "Five-Vertex Lanthanide Coordination on Surfaces: A Route to Sophisticated Nanoarchitectures and Tessellations". In: *J Phys Chem C* 118 (2014), pp. 12908–12915.

[210] N P Kryuchkov et al. "Complex crystalline structures in a two-dimensional core-softened system". In: *Soft Matter* 14 (2018), p. 2152.

[211] Bai-Qiao Song et al. "Periodic tiling of triangular and square nanotubes in a cationic metal – organic framework for selective anion exchange †". In: *Chem Commun* 51 (2015), pp. 9515–9518.

[212] William D Piñeros, Michael Baldea, and Thomas M Truskett. "Designing convex repulsive pair potentials that favor assembly of kagome and snub square lattices". In: *J. Chem. Phys.* 145 (2016), p. 054901.

[213] Mia Baise et al. "Negative Hydration Expansion in ZrW2O8 : Microscopic Mechanism, Spaghetti Dynamics, and Negative Thermal Expansion". In: *Phys. Rev. Lett.* 120 (2018), p. 265501.

[214] V A Gorbunov, S S Akimenko, and A V Myshlyavtsev. "Cross-impact of surface and interaction anisotropy in the self-assembly of organic adsorption monolayers : a Monte Carlo". In: *Phys Chem Chem Phys* 19 (2017), pp. 17111–17120.

[215] Damien Nieckarz, Wojciech Rzysko, and Paweł Szabelski. "On-surface self-assembly of tetratopic molecular building blocks". In: *Phys Chem Chem Phys* 20 (2018), p. 23363.

[216] C Buzano et al. "Two-dimensional lattice-fluid model with waterlike anomalies". In: *Phys. Rev. E* 69 (2004), p. 061502.

[217] Philip J Camp. “Structure and phase behavior of a two-dimensional system with core-softened and long-range repulsive interactions”. In: *Phys. Rev. E* 68 (2003), p. 061506.

[218] Michael Griebel and Jan Hamaekers. “Molecular dynamics simulations of boron-nitride nanotubes embedded in amorphous Si-B-N”. In: *Comput. Mater. Sci.* 39 (2007), pp. 502–517.

[219] Arkadiy Simonov et al. “Hidden diversity of vacancy networks in Prussian blue analogues”. In: *Nature* 578 (2020), p. 256.

[220] Marian Florescu, Salvatore Torquato, and Paul J Steinhardt. “Designer disordered materials with large, complete photonic band gaps”. In: *PNAS* 106.49 (2009), pp. 20658–20663.

[221] Steven R Sellers et al. “Local self-uniformity in photonic networks”. In: *Nat. Commun.* 8 (2017), p. 14439.

[222] Larry Wasserman. “Topological Data Analysis”. In: *Annu. Rev. Stat. Appl.* 5 (2018), p. 501.

[223] Herbert Edelsbrunner and John Harer. “Persistent homology - a survey”. In: *Contemp. Math.* 453 (2008), p. 257.

[224] Benjamin M G D Carter et al. “Structural covariance in the hard sphere fluid”. In: *J. Chem. Phys.* 148 (2018), p. 204511.

[225] V Robins et al. “Pore configuration landscape of granular crystallization”. In: *Nat. Commun.* 8.May (2017), pp. 1–11.

[226] Fei Jiang, Takeshi Tsuji, and Tomoyuki Shirai. “Pore Geometry Characterization by Persistent Homology Theory”. In: *Water Resour. Res.* 54 (2018), pp. 4150–4163.

[227] Lee Steinberg, John Russo, and Jeremy Frey. “A new topological descriptor for water network structure”. In: *J. Cheminform.* 11.48 (2019), pp. 1–11.

[228] Kelin Xia et al. “Persistent Homology for the Quantitative Prediction of Fullerene Stability”. In: *J. Comput. Chem.* 36 (2015), pp. 408–422.

[229] Yasuaki Hiraoka et al. “Hierarchical structures of amorphous solids characterized by persistent homology”. In: *PNAS* 113.26 (2016), pp. 7035–7040.

[230] Yohei Onodera et al. “Understanding diffraction patterns of glassy, liquid and amorphous materials via persistent homology analyses”. In: *J. Ceram. Soc. Japan* 127.12 (2019), pp. 853–863.

[231] Takenobu Nakamura et al. “Persistent homology and many-body atomic structure for medium-range order in the glass”. In: *Nanotechnology* 26 (2015), p. 304001.

[232] Abraham Gutierrez, Mickaël Buchet, and Sylvain Clair. “Persistent Homology To Quantify the Quality of Surface- Supported Covalent Networks”. In: *ChemPhysChem* 20 (2019), pp. 1–7.

[233] The GUDHI Project. *GUDHI User and Reference Manual.* 3.2.0. GUDHI Editorial Board, 2020.

[234] Ulderico Fugacci et al. “Persistent homology: a step-by-step introduction for newcomers”. In: *Smart Tools Apps Comput. Graph.* October (2016).

[235] Nina Otter et al. “A roadmap for the computation of persistent homology”. In: *EPJ Data Sci.* 6 (2017), p. 1.

[236] Afra Zomorodian and Gunnar Carlsson. “Computing Persistent Homology”. In: *Discret. Comput Geom* 33 (2005), pp. 249–274.